A Appendix

A.1 Blur in General BSR Scenarios

To further illustrate the prevalence of blur in high-quality real-world images, we provide additional qualitative and quantitative phenomena as support. Qualitatively, we showcase more examples with blur in real-world data from public datasets where existing methods struggle, highlighting the wide usage of various intentional blurring techniques in real-world image scenarios and the challenges faced by recent general BSR methods, as seen in Fig. 12 and Fig. 13. For instance, the images on the left side of Fig. 12 show how background defocus and lens depth of field enhance subject focus and picture depth. Yet, current BSR methods, while improving texture in foreground areas (Fig. 12, 13, right side, odd row), often mismanage blurred areas with incorrect texturization and oversharpening (Fig. 12, 13, right side, even rows), diminishing the intended blur effect and overall image perception. This issue has not yet received enough attention despite advancements achieved by recent methods in general image processing. From a quantitative perspective, we analyzed the prevalence of blur in key super-resolution benchmarks, including DIV2K, Flickr2K, and DIV8K, with findings summarized in Tab. 7. Approximately 20% of high-resolution images in these datasets exhibit blur, further indicating its widespread presence and underscoring the importance of incorporating blur handling into super-resolution models.

Fig. 12: More visual samples of the existing methods on real-world blur data.

Table 7: Blur proportion in commonly used super-resolution benchmark datasets.

Dataset	DIV2K [2]	Flickr2K [38]	DIV8K [21]	All
Blur Amount/Dataset Size	175+22/800+100	606/2560	266/1500	1069/4960
Blur Proportion	21.86%+22.00%	23.67%	17.73%	21.55%

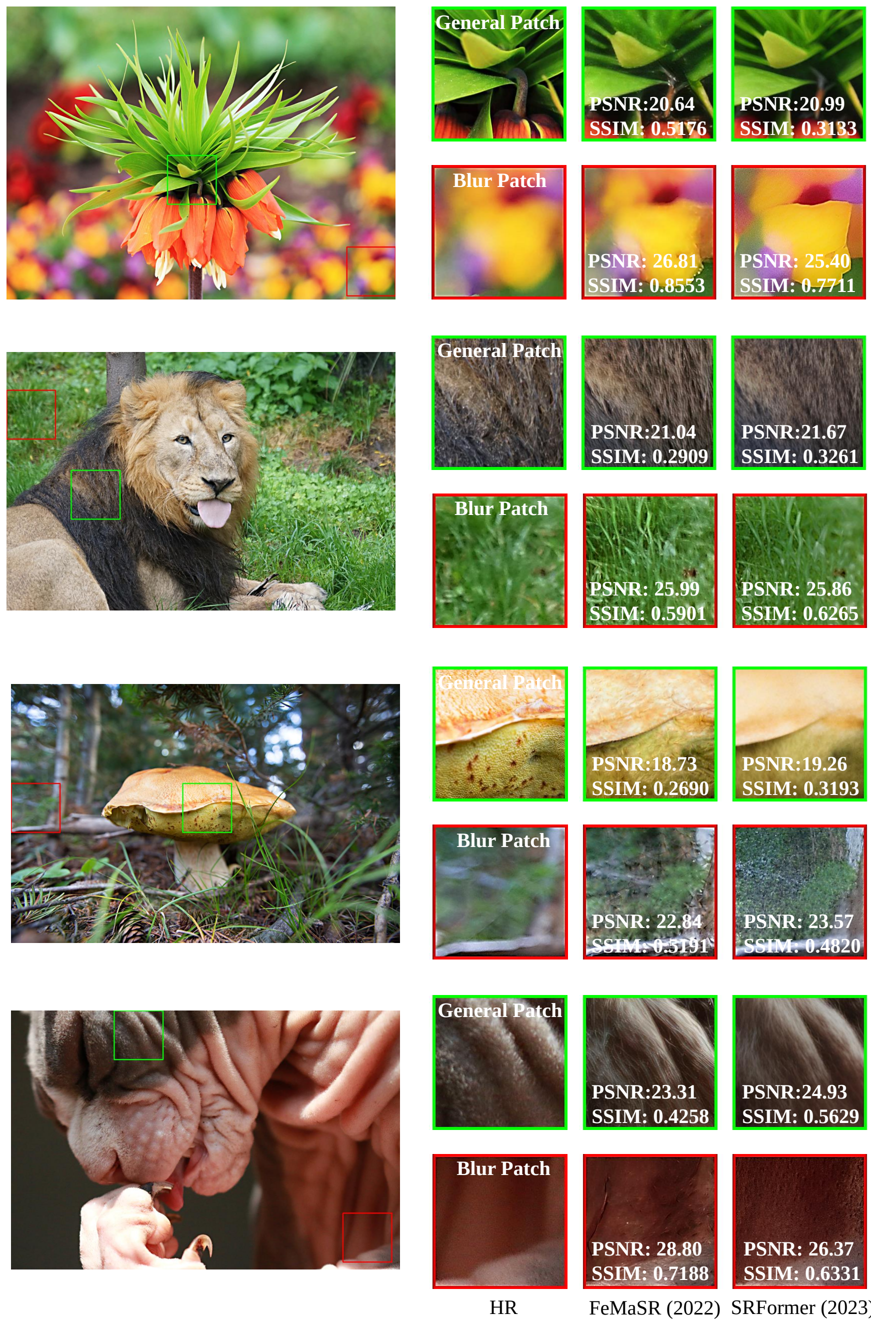

Fig. 13: More visual samples of the existing methods on real-world blur data.

A.2 Effectiveness of Data Synthesis

At first, we synthesized 1000 images that included both defocus and motion blur. However, we found that stable diffusion's understanding of motion blur was more confusing than its effective understanding of defocus blur, and motion blur is often misinterpreted and generated as a defocus blur-like morphology. Therefore, considering the effectiveness of training, we excluded the generated incorrect motion blur from the valid data by manual filtering and supplemented it with a corresponding number of images from online resources. Here, we thoroughly evaluated the quality of the synthesized images from the perspectives of visual effects and quantitative metrics. From a qualitative standpoint, we present a series of synthesized images featuring defocus and motion blur in Fig. 14. Quantitatively, we employed the NIQE [47] as a metric to assess the quality of high-resolution images, comparing the NIQE scores of both real and synthesized samples in ReBlurSR-Train in Fig. 15. The results indicate that the synthetic data exhibits a distribution pattern akin to that of the real data, thereby affirming our process's capability to produce high-quality images that closely mimic the distribution characteristics of authentic data. Additionally, to further validate the effect of synthetic data on model training, we compared the performance of FeMaSR fine-tuned using all data in ReBlurSR-Train and using only the real parts. As shown in Tab. 8, the addition of synthetic data improves the model's LPIPS performance on blur data by about 0.013. This indicates that the synthetic data indeed expands the diversity of the training data and improves the generalization ability.

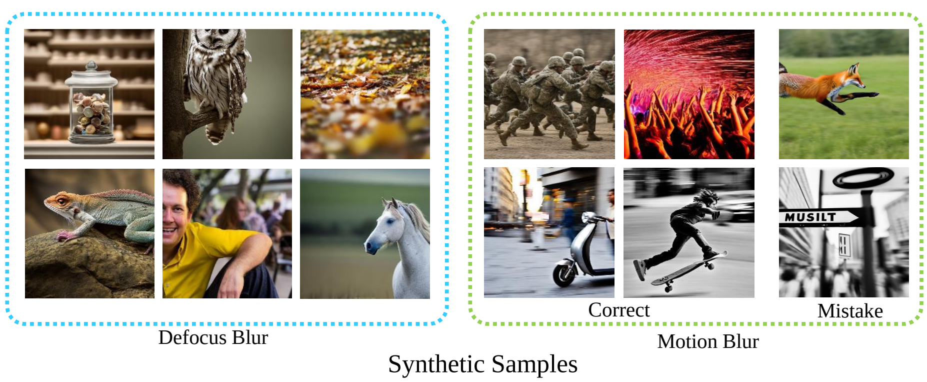

Fig. 14: Samples of synthetic data with different kinds of blur.

A.3 Effectiveness of Cross Fusion Module

To validate the efficacy of the Cross Fusion Model (CFM), we conducted a comparative analysis of various fusion strategies and the fusion proportion. First, as

Table 8: Effectiveness of synthetic data on the blur BSR performance of finetuned FeMaSR (without using general data). 'Real' denotes only the real part of the ReblurSR-Train dataset (old 1804 samples).

Finetuning Data	LPIPS	
	Blur	General
ReBlurSR-Train(Real)	0.3638	**0.4324**
ReblurSR-Train	**0.3508**	0.4388

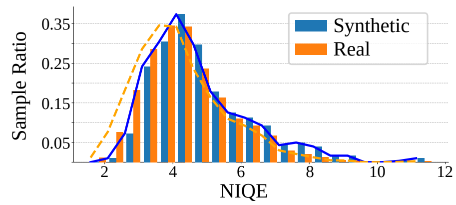

Fig. 15: NIQE distribution comparison between synthetic and real images in the ReBlurSR-Train dataset.

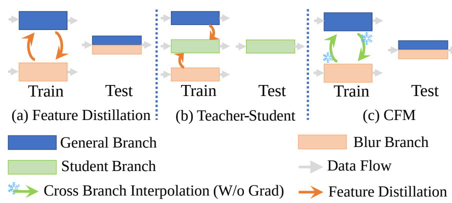

Fig. 16: Different fusion strategies.

Table 9: Comparison of different fusion strategies and proportion of branch fusion. 'BP' denotes back propagation.

Fusion Strategy	Extra BP	LPIPS	
		Blur	General
Feature Distillation	+	0.3674	0.3883
Teacher-Student	+	0.3760	0.3975
CFM	-	**0.3564**	**0.3826**

illustrated in Fig. 16 and Tab. 9, we compared prevalent fusion strategies, encompassing cross feature distillation, the dual-teacher-student framework, and our CFM. Tab. 9 shows that the CFM achieves a 0.006 to 0.008 improvement in LPIPS across all data types compared to the other strategies, without incurring additional computational costs for extra loss and gradient backpropagation, as shown in Fig. 16. This shows the suitability of the model interpolation strategy for SR tasks, enabling CFM to maintain optimal fusion performance with minimal computational loss.

A.4 Discussion about the GAN Artifact Correction (GAC) Methods

To our knowledge, there is some current work [36, 70] aimed at mitigating artifacts in the inference stage of GAN-based image restoration techniques [37, 65], aiming to correct the unnatural appearance of generated textures for greater uniformity and consistency. Notwithstanding their notable achievements in texture correction, they do not pay much attention to the understanding of the disparities between blurred and unblurred data distributions. Consequently, they often neglect to assess the necessity for clear and sharp textures in specific regions, especially the blur regions, still suffering from problems such as edge oversharpening and the generation of inappropriate textures in blurred areas. Essentially, GAN artifact correction strategies and blur image super-resolution pursue divergent objectives: the former seeks to refine the synthesis ed texture, while the latter must discern the appropriateness and necessity of texture synthesis across different image regions, especially in the context of blur data.

For an intuitive comparison, in Tab. 10, we compare our PBaSR framework with prominent GAC methods, including LDL [36] and DeSRA [70], using Real-ESRGAN [65] as the anchor method. As shown, while GAC methods show slight enhancements on blur data, PBaSR achieves a 0.007∼0.02 LPIPS improvement on blur data over LDL and DeSRA, alongside the best performance on general data. Additionally, we show the real sample comparison in Fig. 17. For instance, as depicted on the left side of Fig. 17, LDL and DeSRA struggle with noise (upper right side) and oversharpening (bottom left side) in blurred regions, while our PBaSR adeptly denoises and preserves defocus. Similarly, the sample on the right side of Fig. 17 shows that despite LDL and DeSRA's natural texture synthesis, the over-texturized backgrounds in these examples detract from the blurred region's function of foreground emphasis, compromising overall visual quality. In contrast, PBaSR effectively preserves the blurred region's role in highlighting the subject, thereby enhancing the overall image quality.

In summary, GAN artifact correction methods and blur image blind super-resolution target different objectives—the former improving the synthesized texture and the latter paying more attention to the necessity of texture synthesis in various regions. Integrating the methodologies of these two objectives may be a promising avenue for enhancing outcomes, which we will probably investigate in future research.

Table 10: Comparison of PBaSR with recent GAN Artifact Correction methods on diffrent benchmarks. The best is in bold.

Data	Method	LPIPS ↓	AHIQ ↑	DISTS ↓	VIF ↑	GMSD ↓	VSI ↑
Defocus Blur	Real-ESRGAN (2021)	0.4199	0.2215	0.2313	0.0842	0.1900	0.9547
	$\text{LDL}_{\text{ESRGAN}}$(2022)	0.4333	0.2111	0.2434	0.0827	0.1909	0.9538
	$\text{DeSRA}_{\text{ESRGAN}}$(2023)	0.4186	0.2034	0.2416	0.0871	0.1865	0.9569
	$\text{PBaSR}_{\text{ESRGAN}}$	**0.3986**	**0.2386**	**0.1952**	**0.0907**	**0.1773**	**0.9609**
Motion Blur	Real-ESRGAN (2021)	0.4104	0.2920	0.2212	0.1135	0.1731	0.9733
	$\text{LDL}_{\text{ESRGAN}}$ (2022)	0.4161	0.2870	0.2283	0.1133	0.1722	0.9724
	$\text{DeSRA}_{\text{ESRGAN}}$(2023)	0.3868	0.2686	0.2193	0.1172	0.1665	0.9741
	$\text{PBaSR}_{\text{ESRGAN}}$	**0.3791**	**0.2986**	**0.1907**	**0.1244**	**0.1648**	**0.9771**
General	Real-ESRGAN (2021)	0.4739	0.2175	0.2712	0.0506	0.2276	0.9421
	$\text{LDL}_{\text{ESRGAN}}$ (2022)	0.4784	0.2096	0.2791	0.0502	0.2304	0.9406
	$\text{DeSRA}_{\text{ESRGAN}}$ (2023)	0.5297	0.1854	0.3348	0.0515	0.2346	0.9417
	$\text{PBaSR}_{\text{ESRGAN}}$	**0.4390**	**0.2348**	**0.2315**	**0.0562**	**0.2108**	**0.9541**

Fig. 17: Visual comparison of PBaSR with recent GAN Artifact Correction methods.

A.5 More Comparison Results

More Quantitative Results For reference, we also provided performance comparison between PBaSR and the state-of-the-art methods on more quantitative metrics, including the PSNR, SSIM, CKDN [82], STLPIPS [17] and TOPIQ-FR [5]. The results are shown in Tab. 11. Additionally, we also provide the detailed comparison results of different methods on each general BSR benchmarks in Tab. 12.

Table 11: Extra Quantitative comparison of the proposed method with state-of-the-art methods on Blur data and General data. The **best** and **second-best** results are bolded in black and red.

Data	Metric	SwinIR (2021)	Real-ESRGAN (2021)	MM-RealSR (2022)	FeMaSR (2022)	CAL-GAN (2023)	HAT (2023)	SRFormer (2023)	$\text{PBaSR}_{\text{ESRGAN}}$	$\text{PBaSR}_{\text{FeMaSR}}$	$\text{PBaSR}_{\text{SRFormer}}$
Defocus Blur	PSNR ↑	23.96	24.07	23.62	23.66	**24.41**	23.61	24.24	**24.57**	24.28	24.11
	SSIM ↑	0.6849	**0.6994**	0.6847	0.6553	**0.7146**	0.6374	0.6920	0.6960	0.6854	0.6686
	CKDN ↑	0.4870	0.4716	0.4778	0.4426	0.4263	0.4900	0.4686	0.4934	**0.5225**	**0.5020**
	STLPIPS ↓	0.2827	0.3016	0.2919	0.3351	0.3044	0.2822	0.2753	0.2820	**0.2442**	**0.2507**
	TOPIQ-FR ↑	0.2467	0.2375	0.2325	0.2072	0.2347	0.2660	0.2533	0.2542	**0.2859**	**0.2825**
Motion Blur	PSNR ↑	25.48	25.62	25.41	24.99	25.18	**26.23**	26.11	**26.39**	26.16	26.00
	SSIM ↑	0.7645	0.7876	0.7845	0.6862	0.7451	**0.8122**	0.7752	**0.7934**	0.7759	0.7523
	CKDN ↑	**0.5490**	0.5379	0.5448	0.5296	0.5110	0.5028	0.5310	**0.5462**	0.5445	0.5413
	STLPIPS ↓	0.2300	0.2174	0.2157	0.3007	0.2777	0.2111	0.2179	**0.1987**	**0.2013**	0.2258
	TOPIQ-FR ↑	0.2608	0.2581	0.2419	0.2585	0.2190	0.2494	0.2638	0.2660	**0.2896**	**0.2802**
DIV2K	PSNR ↑	21.25	20.79	21.37	20.16	**21.91**	21.2	**21.88**	21.82	21.74	21.64
	SSIM ↑	0.5604	0.5425	0.5648	0.5045	**0.5789**	0.5321	**0.5788**	0.5655	0.5648	0.5639
	CKDN ↑	0.5123	0.4840	0.4784	0.4691	0.4498	0.4931	0.4964	**0.5144**	**0.5218**	0.5103
	STLPIPS ↓	0.3224	0.3629	0.4042	0.3727	0.4222	**0.2837**	0.3436	0.3476	**0.2874**	0.3018
	TOPIQ-FR ↑	0.2437	0.2216	0.2107	0.1997	0.2161	0.2672	0.2451	0.2501	**0.2834**	**0.2760**

More Qualitative Results We provide more visual comparison results between PBaSR and the state-of-the-art methods in Fig. 18 and Fig. 19.

Table 12: Detailed metrics comparison with state-of-the-art methods on each general BSR benchmarks. The **best** and **second-best** results are bolded in black and red.

Data	Metric	SwinIR (2021)	Real-ESRGAN (2021)	MM-RealSR (2022)	FeMaSR (2022)	CAL-GAN (2023)	HAT (2023)	SRFormer (2023)	$\mathrm{PBaSR_{ESRGAN}}$	$\mathrm{PBaSR_{FeMaSR}}$	$\mathrm{PBaSR_{SRFormer}}$
Urban100	LPIPS ↓	0.4248	0.4994	0.5373	0.4234	0.5137	0.5078	0.4249	0.4675	**0.4155**	**0.3982**
	AHIQ ↑	0.1913	0.1675	0.1640	0.1638	0.1413	0.1847	**0.2094**	0.1734	0.1918	**0.2245**
	DISTS ↓	**0.2501**	0.3056	0.3394	0.2709	0.3174	0.3235	0.2587	0.2955	0.2746	**0.2390**
	VIF ↑	0.0724	0.0622	0.0608	0.0662	0.0594	0.0676	**0.0776**	0.0669	0.0728	**0.0766**
	GMSD ↓	0.2659	0.2832	0.2855	**0.2494**	0.2710	0.2820	0.2653	0.2671	0.2558	**0.2481**
	VSI ↑	0.9028	0.8871	0.8849	**0.9146**	0.8966	0.8864	0.9049	0.9037	0.9131	**0.9159**
BSDS100	LPIPS ↓	0.4691	0.5176	0.5410	0.4479	0.5210	0.5411	0.4987	0.5022	**0.4387**	**0.4442**
	AHIQ ↑	0.1557	0.1711	0.1536	0.1862	0.1386	0.1760	0.1641	0.1673	**0.2016**	**0.1998**
	DISTS ↓	0.3067	0.3387	0.3382	**0.2612**	0.3513	0.3625	0.3240	0.2910	**0.2674**	0.2687
	VIF ↑	0.0428	0.0394	0.0394	0.0438	0.0400	0.0407	0.0437	0.0448	**0.0460**	**0.0454**
	GMSD ↓	0.2205	0.2307	0.2333	**0.2075**	0.2185	0.2375	0.2264	0.2146	0.2104	**0.2079**
	VSI ↑	0.9001	0.8921	0.8902	**0.9048**	0.8977	0.8858	0.8962	0.8989	0.9043	**0.9047**
manga109	LPIPS ↓	0.3714	0.3968	0.4194	**0.3443**	0.4007	0.4175	0.3744	0.3849	**0.3346**	0.3488
	AHIQ ↑	0.2032	0.2010	0.1649	0.1880	0.1542	0.1704	0.1972	0.1743	**0.2230**	**0.2159**
	DISTS ↓	0.2001	0.2225	0.2448	0.1956	0.2200	0.2458	0.2117	0.2185	**0.1851**	**0.1866**
	VIF ↑	0.0850	0.0732	0.0725	0.0799	0.0724	0.0770	**0.0881**	0.0776	**0.0867**	0.0862
	GMSD ↓	0.2526	0.2641	0.2655	**0.2351**	0.2563	0.2590	0.2523	0.2474	**0.2376**	0.2391
	VSI ↑	0.9204	0.9123	0.9099	**0.9284**	0.9149	0.9139	0.9218	0.9219	**0.9289**	0.9282
Set14	LPIPS ↓	0.4398	0.4697	0.4755	0.4033	0.4520	0.4667	0.4394	0.4495	**0.3944**	**0.3971**
	AHIQ ↑	0.1521	0.1600	0.1407	0.1736	0.1393	0.1572	0.1622	0.1486	**0.2017**	**0.1841**
	DISTS ↓	0.2723	0.2814	0.2982	0.2461	0.2803	0.3063	0.2901	0.2639	**0.2439**	**0.2343**
	VIF ↑	0.0625	0.0600	0.0605	0.0621	0.0600	0.0622	**0.0663**	0.0625	0.0659	**0.0663**
	GMSD ↓	0.2360	0.2466	0.2464	**0.2198**	0.2344	0.2397	0.2336	0.2298	0.2223	**0.2189**
	VSI ↑	0.9028	0.8923	0.8918	**0.9064**	0.9021	0.8921	0.9019	0.9034	**0.9062**	0.9108
Set5	LPIPS ↓	0.3998	0.4723	0.4874	0.3611	0.4794	0.4726	0.4679	0.3772	**0.3510**	**0.3512**
	AHIQ ↑	**0.2125**	**0.2227**	0.1184	0.1592	0.2005	0.1984	0.1447	0.1850	0.2083	0.1541
	DISTS ↓	0.3007	0.3571	0.3668	**0.2636**	0.3723	0.3574	0.3562	0.2822	0.2778	**0.2728**
	VIF ↑	0.0628	0.0568	0.0565	0.0586	0.0559	0.0603	**0.0647**	0.0614	0.0638	**0.0661**
	GMSD ↓	0.2255	0.2478	0.2482	**0.2170**	0.2365	0.2454	0.2462	0.2258	**0.2203**	0.2207
	VSI ↑	0.9169	0.9094	0.9118	0.9104	0.9057	0.9098	0.9165	**0.9191**	**0.9174**	0.9171
DIV2K	LPIPS ↓	0.4181	0.4739	0.4929	**0.3848**	0.4847	0.4828	0.4170	0.4390	**0.3826**	0.3892
	AHIQ ↑	0.2311	0.2175	0.2075	0.2396	0.1888	0.2039	0.2329	0.2348	**0.2621**	**0.2579**
	DISTS ↓	0.2314	0.2712	0.3050	**0.1928**	0.2869	0.3186	0.2478	0.2315	0.2059	**0.1966**
	VIF ↑	0.0567	0.0506	0.0504	0.0561	0.0504	0.0519	0.0587	0.0562	**0.0602**	**0.0595**
	GMSD ↓	0.2155	0.2276	0.2303	**0.1976**	0.2215	0.2320	0.2164	0.2108	**0.2003**	0.2017
	VSI ↑	0.9487	0.9421	0.9399	**0.9581**	0.9484	0.9389	0.9485	0.9541	**0.9590**	0.9574
All	LPIPS ↓	0.4202	0.4703	0.4952	0.3986	0.4775	0.4850	0.4284	0.4463	**0.3912**	**0.3937**
	AHIQ ↑	0.1944	0.1890	0.1707	0.1932	0.1557	0.1828	0.1990	0.1860	**0.2190**	**0.2223**
	DISTS ↓	0.2475	0.2839	0.3060	**0.2303**	0.2928	0.3115	0.2615	0.2587	0.2331	**0.2229**
	VIF ↑	0.0646	0.0568	0.0563	0.0619	0.0560	0.0598	**0.0674**	0.0617	0.0668	**0.0673**
	GMSD ↓	0.2387	0.2515	0.2536	**0.2225**	0.2418	0.2523	0.2402	0.2350	0.2261	**0.2243**
	VSI ↑	0.9176	0.9080	0.9059	0.9257	0.9139	0.9060	0.9174	0.9192	**0.9257**	**0.9260**

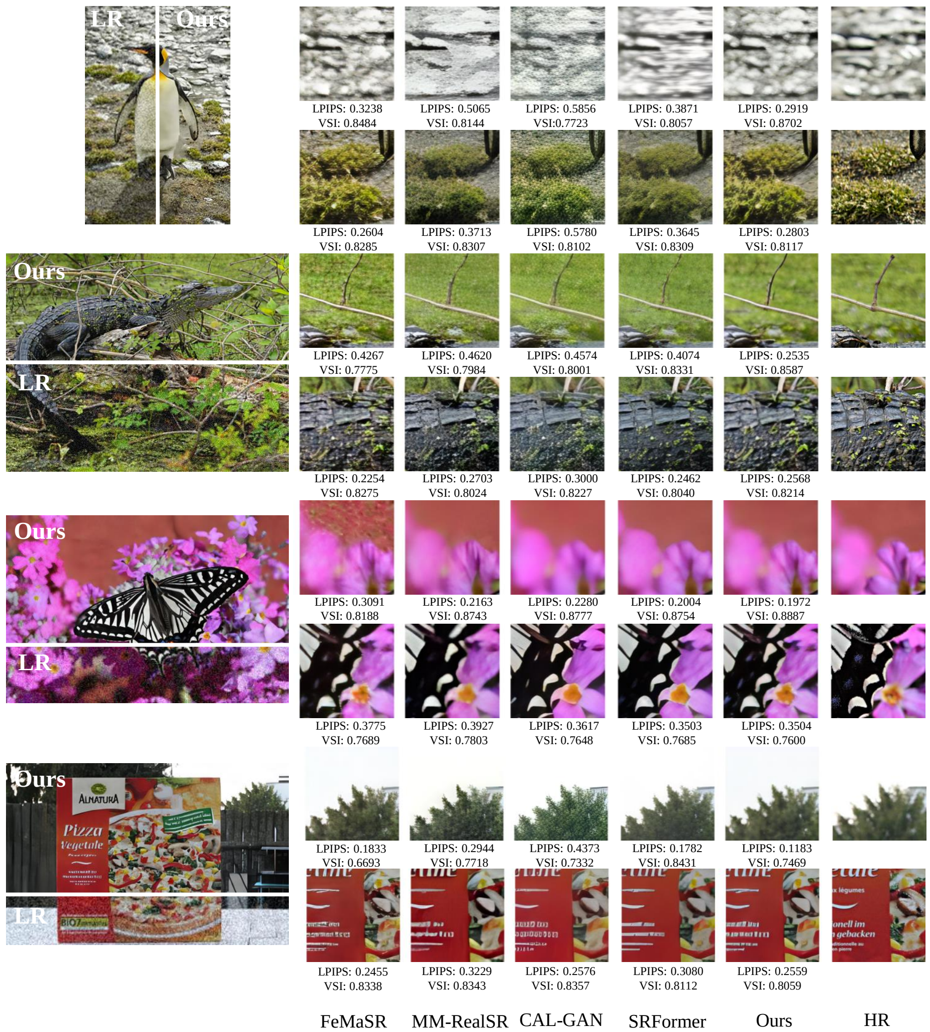

Fig. 18: More visual comparison of the proposed method with state-of-the-art methods on blur data.

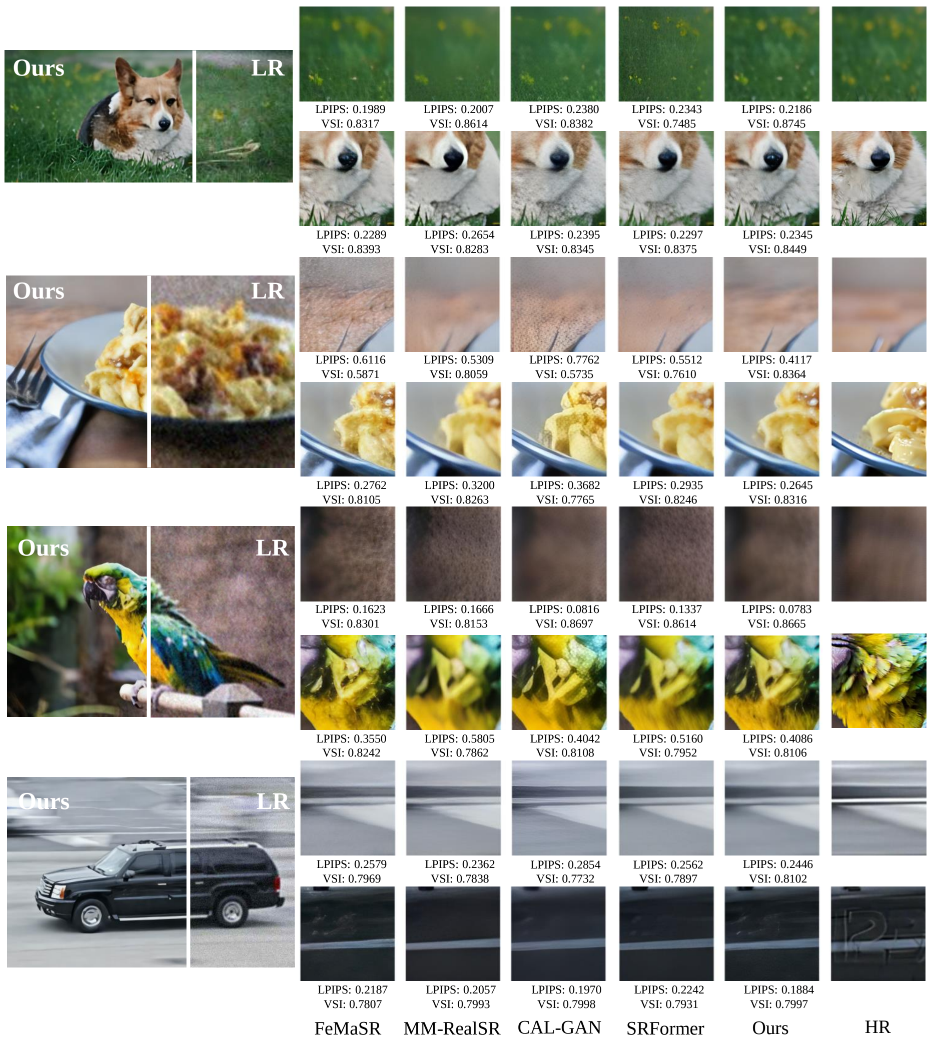

Fig. 19: More Visual comparison of the proposed method with state-of-the-art methods on blur data.

References

1. Abuolaim, A., Brown, M.S.: Defocus deblurring using dual-pixel data. In: Computer Vision–ECCV 2020: 16th European Conference, Glasgow, UK, August 23–28, 2020, Proceedings, Part X 16. pp. 111–126. Springer (2020)
2. Agustsson, E., Timofte, R.: Ntire 2017 challenge on single image super-resolution: Dataset and study. In: The IEEE Conference on Computer Vision and Pattern Recognition (CVPR) Workshops (July 2017) 1
3. Bevilacqua, M., Roumy, A., Guillemot, C.M., Alberi-Morel, M.L.: Low-complexity single-image super-resolution based on nonnegative neighbor embedding. In: British Machine Vision Conference (2012), https://api.semanticscholar.org/CorpusID:5250573
4. Chen, C., Li, X., Yang, L., Lin, X., Zhang, L., Wong, K.Y.K.: Progressive semantic-aware style transformation for blind face restoration. In: Proceedings of the IEEE/CVF conference on computer vision and pattern recognition. pp. 11896–11905 (2021)
5. Chen, C., Mo, J., Hou, J., Wu, H., Liao, L., Sun, W., Yan, Q., Lin, W.: Topiq: A top-down approach from semantics to distortions for image quality assessment. arXiv preprint arXiv:2308.03060 (2023) 6
6. Chen, C., Shi, X., Qin, Y., Li, X., Han, X., Yang, T., Guo, S.: Real-world blind super-resolution via feature matching with implicit high-resolution priors. In: Proceedings of the 30th ACM International Conference on Multimedia. pp. 1329–1338 (2022)
7. Chen, H., Hao, J., Zhao, K., Yuan, K., Sun, M., Zhou, C., Hu, W.: Cassr: Activating image power for real-world image super-resolution. arXiv preprint arXiv:2403.11451 (2024)
8. Chen, J., Li, B., Xue, X.: Scene text telescope: Text-focused scene image super-resolution. In: Proceedings of the IEEE/CVF Conference on Computer Vision and Pattern Recognition (CVPR). pp. 12026–12035 (June 2021)
9. Chen, X., Wang, X., Zhou, J., Qiao, Y., Dong, C.: Activating more pixels in image super-resolution transformer. In: Proceedings of the IEEE/CVF Conference on Computer Vision and Pattern Recognition (CVPR). pp. 22367–22377 (June 2023)
10. Chen, Z., Wu, Z., Zamfir, E., Zhang, K., Zhang, Y., Timofte, R., Yang, X., Yu, H., Wan, C., Hong, Y., et al.: Ntire 2024 challenge on image super-resolution (x4): Methods and results. In: Proceedings of the IEEE/CVF Conference on Computer Vision and Pattern Recognition. pp. 6108–6132 (2024)
11. Cho, S.J., Ji, S.W., Hong, J.P., Jung, S.W., Ko, S.J.: Rethinking coarse-to-fine approach in single image deblurring. In: Proceedings of the IEEE/CVF international conference on computer vision. pp. 4641–4650 (2021)
12. Ding, K., Ma, K., Wang, S., Simoncelli, E.P.: Image quality assessment: Unifying structure and texture similarity. CoRR **abs/2004.07728** (2020), https://arxiv.org/abs/2004.07728
13. Ding, K., Ma, K., Wang, S., Simoncelli, E.P.: Comparison of full-reference image quality models for optimization of image processing systems. International Journal of Computer Vision **129**, 1258–1281 (2021)
14. Dong, C., Loy, C.C., He, K., Tang, X.: Learning a deep convolutional network for image super-resolution. In: Computer Vision–ECCV 2014: 13th European Conference, Zurich, Switzerland, September 6-12, 2014, Proceedings, Part IV 13. pp. 184–199. Springer (2014)

15. Dong, C., Loy, C.C., He, K., Tang, X.: Image super-resolution using deep convolutional networks. IEEE transactions on pattern analysis and machine intelligence **38**(2), 295–307 (2015)
16. Fritsche, M., Gu, S., Timofte, R.: Frequency separation for real-world super-resolution. In: 2019 IEEE/CVF International Conference on Computer Vision Workshop (ICCVW). pp. 3599–3608. IEEE (2019)
17. Ghildyal, A., Liu, F.: Shift-tolerant perceptual similarity metric. In: European Conference on Computer Vision (2022) 6
18. Gong, Y., Liao, P., Zhang, X., Zhang, L., Chen, G., Zhu, K., Tan, X., Lv, Z.: Enlighten-gan for super resolution reconstruction in mid-resolution remote sensing images. Remote Sensing **13**(6), 1104 (2021)
19. Google Chrome team, F.B.: Blur camera background (2023), https://developer.chrome.com/blog/background-blur?hl=zh-cn
20. Gu, J., Lu, H., Zuo, W., Dong, C.: Blind super-resolution with iterative kernel correction. In: Proceedings of the IEEE/CVF Conference on Computer Vision and Pattern Recognition. pp. 1604–1613 (2019)
21. Gu, S., Lugmayr, A., Danelljan, M., Fritsche, M., Lamour, J., Timofte, R.: Div8k: Diverse 8k resolution image dataset. In: 2019 IEEE/CVF International Conference on Computer Vision Workshop (ICCVW). pp. 3512–3516. IEEE (2019) 1
22. Hinton, G., Vinyals, O., Dean, J.: Distilling the knowledge in a neural network. arXiv preprint arXiv:1503.02531 (2015)
23. Hore, A., Ziou, D.: Image quality metrics: Psnr vs. ssim. In: 2010 20th international conference on pattern recognition. pp. 2366–2369. IEEE (2010)
24. Horé, A., Ziou, D.: Image quality metrics: Psnr vs. ssim. In: 2010 20th International Conference on Pattern Recognition. pp. 2366–2369 (2010). https://doi.org/10.1109/ICPR.2010.579
25. Huang, G., Liu, Z., Van Der Maaten, L., Weinberger, K.Q.: Densely connected convolutional networks. In: Proceedings of the IEEE conference on computer vision and pattern recognition. pp. 4700–4708 (2017)
26. Huang, J.B., Singh, A., Ahuja, N.: Single image super-resolution from transformed self-exemplars. In: Proceedings of the IEEE Conference on Computer Vision and Pattern Recognition (CVPR) (June 2015)
27. Huang, Y., Li, S., Wang, L., Tan, T., et al.: Unfolding the alternating optimization for blind super resolution. Advances in Neural Information Processing Systems **33**, 5632–5643 (2020)
28. Ji, X., Cao, Y., Tai, Y., Wang, C., Li, J., Huang, F.: Real-world super-resolution via kernel estimation and noise injection. In: proceedings of the IEEE/CVF conference on computer vision and pattern recognition workshops. pp. 466–467 (2020)
29. Jin, Y., Qian, M., Xiong, J., Xue, N., Xia, G.S.: Depth and dof cues make a better defocus blur detector. arXiv preprint arXiv:2306.11334 (2023)
30. Jin, Y., Qian, M., Xiong, J., Xue, N., Xia, G.S.: Depth and dof cues make a better defocus blur detector. arXiv preprint arXiv:2306.11334 (2023)
31. Kim, B., Son, H., Park, S.J., Cho, S., Lee, S.: Defocus and motion blur detection with deep contextual features. In: Computer Graphics Forum. vol. 37, pp. 277–288. Wiley Online Library (2018)
32. Kim, J., Lee, J.K., Lee, K.M.: Deeply-recursive convolutional network for image super-resolution. In: Proceedings of the IEEE conference on computer vision and pattern recognition. pp. 1637–1645 (2016)
33. Lao, S., Gong, Y., Shi, S., Yang, S., Wu, T., Wang, J., Xia, W., Yang, Y.: Attentions help cnns see better: Attention-based hybrid image quality assessment network. arXiv preprint arXiv:2204.10485 (2022)

34. Li, X., Chen, C., Zhou, S., Lin, X., Zuo, W., Zhang, L.: Blind face restoration via deep multi-scale component dictionaries. In: European conference on computer vision. pp. 399–415. Springer (2020)
35. Li, X., Li, W., Ren, D., Zhang, H., Wang, M., Zuo, W.: Enhanced blind face restoration with multi-exemplar images and adaptive spatial feature fusion. In: Proceedings of the IEEE/CVF Conference on Computer Vision and Pattern Recognition. pp. 2706–2715 (2020)
36. Liang, J., Zeng, H., Zhang, L.: Details or artifacts: A locally discriminative learning approach to realistic image super-resolution. In: Proceedings of the IEEE Conference on Computer Vision and Pattern Recognition (2022) 4, 5
37. Liang, J., Cao, J., Sun, G., Zhang, K., Van Gool, L., Timofte, R.: Swinir: Image restoration using swin transformer. In: Proceedings of the IEEE/CVF international conference on computer vision. pp. 1833–1844 (2021) 4
38. Lim, B., Son, S., Kim, H., Nah, S., Mu Lee, K.: Enhanced deep residual networks for single image super-resolution. In: Proceedings of the IEEE conference on computer vision and pattern recognition workshops. pp. 136–144 (2017) 1
39. Liu, G., Ding, Y., Li, M., Sun, M., Wen, X., Wang, B.: Reconstructed convolution module based look-up tables for efficient image super-resolution. In: Proceedings of the IEEE/CVF International Conference on Computer Vision. pp. 12217–12226 (2023)
40. Liu, H., Wu, M., Yuan, K., Sun, M., Tang, Y., Zheng, C., Wen, X., Li, X.: Ada-dqa: Adaptive diverse quality-aware feature acquisition for video quality assessment. In: Proceedings of the 31st ACM International Conference on Multimedia. p. 6695–6704. Association for Computing Machinery (2023)
41. Lu, Y., Li, X., Pei, Y., Yuan, K., Xie, Q., Qu, Y., Sun, M., Zhou, C., Chen, Z.: Kvq: Kaleidoscope video quality assessment for short-form videos. arXiv preprint arXiv:2402.07220 (2024)
42. Ma, C., Yang, C.Y., Yang, X., Yang, M.H.: Learning a no-reference quality metric for single-image super-resolution. Computer Vision and Image Understanding **158**, 1–16 (2017)
43. Martin, D., Fowlkes, C., Tal, D., Malik, J.: A database of human segmented natural images and its application to evaluating segmentation algorithms and measuring ecological statistics. In: Proceedings Eighth IEEE International Conference on Computer Vision. ICCV 2001. vol. 2, pp. 416–423. IEEE (2001)
44. Matsui, Y., Ito, K., Aramaki, Y., Fujimoto, A., Ogawa, T., Yamasaki, T., Aizawa, K.: Sketch-based manga retrieval using manga109 dataset. Multimedia Tools and Applications **76**, 21811–21838 (2017)
45. Menon, S., Damian, A., Hu, S., Ravi, N., Rudin, C.: Pulse: Self-supervised photo upsampling via latent space exploration of generative models. In: Proceedings of the ieee/cvf conference on computer vision and pattern recognition. pp. 2437–2445 (2020)
46. Mittal, A., Soundararajan, R., Bovik, A.C.: Making a "completely blind" image quality analyzer. IEEE Signal processing letters **20**(3), 209–212 (2012)
47. Mittal, A., Soundararajan, R., Bovik, A.C.: Making a "completely blind" image quality analyzer. IEEE Signal Processing Letters **20**(3), 209–212 (2013). https://doi.org/10.1109/LSP.2012.2227726 3
48. Mou, C., Wu, Y., Wang, X., Dong, C., Zhang, J., Shan, Y.: Metric learning based interactive modulation for real-world super-resolution. In: European Conference on Computer Vision (ECCV) (2022)
49. OpenAI: Chatgpt: Optimizing language models for dialogue. https://openai.com/chatgpt (2023), accessed: 2024-01-18

50. Pan, X., Zhan, X., Dai, B., Lin, D., Loy, C.C., Luo, P.: Exploiting deep generative prior for versatile image restoration and manipulation. IEEE Transactions on Pattern Analysis and Machine Intelligence **44**(11), 7474–7489 (2021)
51. Park, J., Son, S., Lee, K.M.: Content-aware local gan for photo-realistic super-resolution. In: Proceedings of the IEEE/CVF International Conference on Computer Vision. pp. 10585–10594 (2023)
52. Qin, R., Sun, M., Zhang, F., Wen, X., Wang, B.: Blind image super-resolution with rich texture-aware codebook. In: Proceedings of the 31st ACM International Conference on Multimedia. pp. 676–687 (2023)
53. Qin, R., Wang, B., Tai, Y.W.: Scene text image super-resolution via content perceptual loss and criss-cross transformer blocks. arXiv preprint arXiv:2210.06924 (2022)
54. Qu, Y., Yuan, K., Zhao, K., Xie, Q., Hao, J., Sun, M., Zhou, C.: Xpsr: Cross-modal priors for diffusion-based image super-resolution. arXiv preprint arXiv:2403.05049 (2024)
55. Rombach, R., Blattmann, A., Lorenz, D., Esser, P., Ommer, B.: High-resolution image synthesis with latent diffusion models (2021)
56. Sheikh, H.R., Bovik, A.C.: Image information and visual quality. IEEE Transactions on image processing **15**(2), 430–444 (2006)
57. Shi, J., Xu, L., Jia, J.: Discriminative blur detection features. In: Proceedings of the IEEE Conference on Computer Vision and Pattern Recognition. pp. 2965–2972 (2014)
58. Shi, W., Caballero, J., Huszár, F., Totz, J., Aitken, A.P., Bishop, R., Rueckert, D., Wang, Z.: Real-time single image and video super-resolution using an efficient sub-pixel convolutional neural network. In: Proceedings of the IEEE conference on computer vision and pattern recognition. pp. 1874–1883 (2016)
59. Soundararajan, R., Bovik, A.C.: Rred indices: Reduced reference entropic differencing for image quality assessment. IEEE Transactions on Image Processing **21**(2), 517–526 (2011)
60. Tang, C., Liu, X., Zheng, X., Li, W., Xiong, J., Wang, L., Zomaya, A.Y., Longo, A.: Defusionnet: Defocus blur detection via recurrently fusing and refining discriminative multi-scale deep features. IEEE Transactions on Pattern Analysis and Machine Intelligence **44**(2), 955–968 (2020)
61. Tang, C., Liu, X., Zhu, X., Zhu, E., Sun, K., Wang, P., Wang, L., Zomaya, A.: R^2mrf: Defocus blur detection via recurrently refining multi-scale residual features. In: Proceedings of the AAAI Conference on Artificial Intelligence. vol. 34, pp. 12063–12070 (2020)
62. team, A.P.L.: Photography tips: when to use a large aperture. (2024), https://www.adobe.com/creativecloud/photography/hub /guides/when-to-use-large-aperture.html
63. Wang, J., Yang, Z., Hu, X., Li, L., Lin, K., Gan, Z., Liu, Z., Liu, C., Wang, L.: Git: A generative image-to-text transformer for vision and language. arXiv preprint arXiv:2205.14100 (2022)
64. Wang, L., Wang, Y., Dong, X., Xu, Q., Yang, J., An, W., Guo, Y.: Unsupervised degradation representation learning for blind super-resolution. In: Proceedings of the IEEE/CVF Conference on Computer Vision and Pattern Recognition. pp. 10581–10590 (2021)
65. Wang, X., Xie, L., Dong, C., Shan, Y.: Real-esrgan: Training real-world blind super-resolution with pure synthetic data. In: Proceedings of the IEEE/CVF international conference on computer vision. pp. 1905–1914 (2021) 4, 5

66. Wang, X., Yu, K., Wu, S., Gu, J., Liu, Y., Dong, C., Qiao, Y., Change Loy, C.: Esrgan: Enhanced super-resolution generative adversarial networks. In: Proceedings of the European conference on computer vision (ECCV) workshops. pp. 0–0 (2018)
67. Wang, Z., Bovik, A.C., Sheikh, H.R., Simoncelli, E.P.: Image quality assessment: from error visibility to structural similarity. IEEE transactions on image processing **13**(4), 600–612 (2004)
68. Wu, Y., Wang, X., Li, G., Shan, Y.: Animesr: learning real-world super-resolution models for animation videos. Advances in Neural Information Processing Systems **35**, 11241–11252 (2022)
69. Xiao, Y., Yuan, Q., Jiang, K., He, J., Wang, Y., Zhang, L.: From degrade to upgrade: Learning a self-supervised degradation guided adaptive network for blind remote sensing image super-resolution. Information Fusion **96**, 297–311 (2023)
70. Xie, L., Wang, X., Chen, X., Li, G., Shan, Y., Zhou, J., Dong, C.: Desra: Detect and delete the artifacts of gan-based real-world super-resolution models. In: Proceedings of the 40th International Conference on Machine Learning. ICML'23 (2023) 4, 5
71. Xue, W., Zhang, L., Mou, X., Bovik, A.C.: Gradient magnitude similarity deviation: A highly efficient perceptual image quality index. IEEE transactions on image processing **23**(2), 684–695 (2013)
72. Yuan, K., Kong, Z., Zheng, C., Sun, M., Wen, X.: Capturing co-existing distortions in user-generated content for no-reference video quality assessment. In: Proceedings of the 31st ACM International Conference on Multimedia. p. 1098–1107. Association for Computing Machinery (2023)
73. Yuan, K., Liu, H., Li, M., Sun, M., Sun, M., Gong, J., Hao, J., Zhou, C., Tang, Y.: Ptm-vqa: Efficient video quality assessment leveraging diverse pretrained models from the wild. In: Proceedings of the IEEE/CVF Conference on Computer Vision and Pattern Recognition (CVPR). pp. 2835–2845 (June 2024)
74. Zeyde, R., Elad, M., Protter, M.: On single image scale-up using sparse-representations. In: Curves and Surfaces: 7th International Conference, Avignon, France, June 24-30, 2010, Revised Selected Papers 7. pp. 711–730. Springer (2012)
75. Zhang, K., Liang, J., Van Gool, L., Timofte, R.: Designing a practical degradation model for deep blind image super-resolution. In: Proceedings of the IEEE/CVF International Conference on Computer Vision. pp. 4791–4800 (2021)
76. Zhang, L., Shen, Y., Li, H.: Vsi: A visual saliency-induced index for perceptual image quality assessment. IEEE Transactions on Image Processing **23**(10), 4270–4281 (2014). https://doi.org/10.1109/TIP.2014.2346028
77. Zhang, R., Isola, P., Efros, A.A., Shechtman, E., Wang, O.: The unreasonable effectiveness of deep features as a perceptual metric. In: Proceedings of the IEEE conference on computer vision and pattern recognition. pp. 586–595 (2018)
78. Zhang, Y., Tian, Y., Kong, Y., Zhong, B., Fu, Y.: Residual dense network for image super-resolution. In: Proceedings of the IEEE conference on computer vision and pattern recognition. pp. 2472–2481 (2018)
79. Zhao, C., Feng, S., Zhao, B.N., Ding, Z., Wu, J., Shen, F., Shen, H.T.: Scene text image super-resolution via parallelly contextual attention network. In: Proceedings of the 29th ACM International Conference on Multimedia. p. 2908–2917 (2021)
80. Zhao, K., Yuan, K., Sun, M., Li, M., Wen, X.: Quality-aware pre-trained models for blind image quality assessment. In: Proceedings of the IEEE/CVF Conference on Computer Vision and Pattern Recognition (CVPR). pp. 22302–22313 (June 2023)

81. Zhao, K., Yuan, K., Sun, M., Wen, X.: Zoom-vqa: Patches, frames and clips integration for video quality assessment. In: Proceedings of the IEEE/CVF Conference on Computer Vision and Pattern Recognition (CVPR) Workshops. pp. 1302–1310 (June 2023)
82. Zheng, H., Yang, H., Fu, J., Zha, Z.J., Luo, J.: Learning conditional knowledge distillation for degraded-reference image quality assessment. In: 2021 IEEE/CVF International Conference on Computer Vision (ICCV). pp. 10222–10231 (2021). https://doi.org/10.1109/ICCV48922.2021.01008 6
83. Zhou, S., Chan, K., Li, C., Loy, C.C.: Towards robust blind face restoration with codebook lookup transformer. Advances in Neural Information Processing Systems **35**, 30599–30611 (2022)
84. Zhou, Y., Li, Z., Guo, C.L., Bai, S., Cheng, M.M., Hou, Q.: Srformer: Permuted self-attention for single image super-resolution. arXiv preprint arXiv:2303.09735 (2023)
85. Zhu, J.Y., Park, T., Isola, P., Efros, A.A.: Unpaired image-to-image translation using cycle-consistent adversarial networks. In: Proceedings of the IEEE international conference on computer vision. pp. 2223–2232 (2017)
86. Zhu, Q., Hao, J., Ding, Y., Liu, Y., Mo, Q., Sun, M., Zhou, C., Zhu, S.: Cpga: Coding priors-guided aggregation network for compressed video quality enhancement. In: Proceedings of the IEEE/CVF Conference on Computer Vision and Pattern Recognition (CVPR). pp. 2964–2974 (June 2024)